IMPROVEMENT OF THE FAST MOVING TARGETS PRESENTATION IN ISAR BY USING THE S-METHOD

LJ. Stanković, T. Thayaparan**, M. Daković**

* Elektrotehnički fakultet, University of Montenegro, Podgorica, Serbia and Montenegro
** Radar Applications and Space Technology, Defence Research and Development, Ottawa, Ontario, Canada

ABSTRACT

Commonly used technique for the ISAR signal analysis is a two dimensional Fourier transform. In the cases when the line of sight projection of target point velocity changes or the movement within the coherent integration time is non-compensated then the Fourier transform produces blurred and distorted images. Standard techniques for these kind of problems are in movement compensation or in the time-frequency analysis application. Both of them are computationaly intensive. Here, we will present a numerically simple S-method based approach. This approach improves readability of ISAR images, with only a slight correction of the existing Fourier transform based algorithms. Implementation is presented and tested on common benchmark signals.

1. INTRODUCTION

When radar transmits an electromagnetic signal to a target, the signal reflects from it and returns to radar. The reflected signal, as compared to the transmitted signal, is delayed, changed in amplitude, and possibly shifted in frequency. These parameters of the received signal contain information about the target's characteristics. For example, delay is related to the target's distance from the radar, while the target's velocity is related to the shift in frequency. Inverse synthetic aperture radar (ISAR) is a method for obtaining high resolution image of a target based on the change in viewing angle of the target with respect to the fixed radar. Common technique used for the ISAR signal analysis is the two dimensional Fourier transform. Fourier transform application on the ISAR signal of a point target results in a highly concentrated function at a point whose position corresponds to the range and cross range values [7, 8]. Within longer time intervals the target point velocity changes, meaning that corresponding frequency changes, that spread Fourier transform, blurring information about the cross range. The rotation itself can be nonconstant, increasing the radar image distortion. In addition to these disturbances in the radar image, target motion can also be three dimensional, changing the velocity projection along the target-radar line in a very complex way. In order to deal with this kind of problems, instead of the standard Fourier transfer, time-frequency representations that can track spectral content in time, should be used. One approach is based on the motion compensation by using adaptive time-frequency representation with additional phase compensation factor [7, 8]. It is computationally extensive. The other approach is based on the usage of the quadratic time-frequency representations [1].

In this paper we propose that instead of the Fourier transform, the S-method based calculation is used. Like the Wigner distribution, this distribution can produce fully concentrated representation for linear changes of the frequency, at the same time being cross-terms free or with significantly reduced cross-terms [3, 4, 5, 6]. Note that this distribution is numerically very simple and requires just few more operations than the standard Fourier transform. This method works on the whole set of data. It does not split the ISAR image into a time series of ISAR images. This is a significant advantage over the other quadratic representations and linear transforms based on signal dechirping and multiparameter search procedures.

2. ANALYTIC CW RADAR SIGNAL MODEL

For the analytic model derivation, consider a continuous wave (CW) radar that transmits signal in a form of coherent series of chirps [1]

$$v_p(t) = \begin{cases} \exp(j\pi B f_r t^2) & \text{for} \quad 0 \le t \le T_r \\ 0 & \text{otherwise} \end{cases} \tag{1}$$

where T_r is the repetition time and $f_r = 1/T_r$ is the repetition frequency and B is the signal bandwidth. In one revisit transmitted signal consists of M such chirps

$$v(t) = \exp(-j\omega_0 t) \sum_{m=0}^{M-1} v_p(t - mT_r),$$

where ω_0 is the radar operating frequency. Total signal duration is $T_c = MT_r$. It is called coherent integration time (CIT). The received signal is mixed (multiplied) with the complex-conjugate of the transmitted signal, shifted in time. One component of the received signal, after a low-pass filtering, is

$$q(m,t) = \sigma \exp(j\omega_0 \frac{2d}{c}) \exp(-j2\pi B f_r (t - mT_r) \frac{2d}{c}), \tag{2}$$

where σ is the reflection coefficient, d is the radar to target distance and c is the propagation (light) speed.

3. FOURIER TRANSFORM IN ISAR

Two-dimensional (2D) Fourier transform of the received signal $q(m,n)$ is

$$Q(m',n') = \sum_{m=0}^{M-1} \sum_{n=0}^{N-1} q(m,n) \exp(-j[2\pi m/M + 2\pi n/N])$$

with $t - mT_r = nT_s$. The periodogram

$$P(m',n') = \left|Q(m',n')\right|^2$$

represents an ISAR image.

In order to analyze cross-range nonstationarities in the Fourier transform, consider only the Doppler component part in the received signal in continuous dwell time of one target point (the $p-th$ point), as it is usually done in the literature on ISAR,

$$e_p(t) = \sigma_p \exp(j \frac{2\omega_0}{c} d_p(t)). \tag{3}$$

The Fourier transform of $e_p(t)$ produces

$$E_p(\omega) = \int_{-\infty}^{\infty} w(t)e_p(t)\exp(-j\omega t)dt,$$

where $w(t)$ is the window defining the considered time interval (CIT). In order to simplify the notation in this part we will just omit the index p.

For time-varying $d(t)$ we can write a Taylor series expansion of $d(t)$ around $t = 0$

$$d(t) = d_0 + d'(0)t + ... = \sum_{n=0}^{\infty} \frac{1}{n!} d^{(n)}(0)t^n \quad (4)$$

where $d^{(n)}(0)$ is the $n-$th derivative of the distance at $t = 0$ and the Doppler shift is

$$\Delta\omega_d = 2\omega_0 d'(0)/c.$$

Fourier transform (FT) of (3) with (4) is of the form

$$E(\omega) = \int_{-\infty}^{\infty} w(t)\exp(j\frac{2\omega_0}{c}\sum_{n=0}^{\infty}\frac{1}{n!}d^{(n)}(0)t^n - j\omega t)dt$$

Now, by omitting the constant term $d(0)$ and with $\Delta\omega_d = 2\omega_0 d'(0)/c$ we get

$$E(\omega) = W(\omega - \Delta\omega_d) *_\omega FT\left[\exp(j\frac{2\omega_0}{c}\sum_{n=2}^{\infty}\frac{1}{n!}d^{(n)}(0)t^n)\right],$$

where $*_\omega$ denotes convolution in frequency. Thus, the Fourier transform is located at and around the Doppler shift $\omega = \Delta\omega_d$. It is spread by the factor $S_{spread}(\omega) = FT\left[\exp(j\frac{2\omega_0}{c}\sum_{n=2}^{\infty}\frac{1}{n!}\Delta d^{(n)}(0)t^n)\right]$ .This factor depends on the derivatives of the distance, starting from the second order (first order derivative of the Doppler shift), i.e., the spread factor depends on

$$s_f(t) = \frac{1}{2}d^{''}(0)t^2 + \frac{1}{6}d'''(0)t^3 + ...$$

It can significantly degrade the periodogram image $P(\omega) = |E(\omega)|^2$.

4. S-METHOD BASED IMPROVEMENT OF THE RADAR IMAGES

Here we will present a method for readability improvement of images blurred due to the long TIC and/or nonuniform movement. Let us, instead of the Fourier transform (periodogram), use the S-method defined by [5, 4]

$$SM(\omega) = \frac{1}{\pi}\int_{-\infty}^{\infty} E(\omega+\theta)E^*(\omega-\theta)d\theta. \quad (5)$$

It can improve the image concentration in a numerically very simple and efficient way. Namely, by replacing $E(\omega)$ into (5) we get

$$SM(\omega) = \frac{1}{\pi}\int_{-\infty}^{\infty}\int_{-\infty}^{\infty}\int_{-\infty}^{\infty} w(t_1)w^*(t_2)$$

$$\times\exp\left[j\frac{2\omega_0}{c}\sum_{n=0}^{\infty}\frac{1}{n!}d^{(n)}(0)t_1^n - j\frac{2\omega_0}{c}\sum_{n=0}^{\infty}\frac{1}{n!}d^{(n)}(0)t_2^n\right]$$

$$\times\exp(-j(\omega+\theta)t_1)\exp(j(\omega-\theta)t_2)dt_1dt_2d\theta.$$

The part of integrand depending on θ is $\exp(-j\theta(t_1+t_2))$. Integration over θ results in $2\pi\delta((t_1+t_2)$. In the previous equation it means that we get

$$SM(\omega) = W_e(\omega - \Delta\omega_d) *_\omega FT\left[\exp(j\frac{2\omega_0}{c}(\frac{1}{3!}d^{'''}(0)t^3 + ...\right]$$

where similar calculations as in the FT case are done.

The S-method based image is located at the same position as the Fourier transform image, $\omega = \Delta\omega_d$, but with the spreading term $S_{spread}(\omega) = FT\left[\exp(j\frac{2\omega_0}{c}(\frac{1}{3!}d^{'''}(0)t^3 + ...\right]$. Its exponent starts from the third derivative $d^{'''}(0)$,

$$s_f(t) = \frac{1}{6}d'''(0)t^3 + \frac{1}{120}d^{(5)}(0)t^5 + ...$$

Recall that in the Fourier transform based image the spreading terms started from the second derivative $d^{''}(0)$. It means that in the S-method, the points with linear Doppler changes

$$\frac{2\omega_0}{c}d'(t) = \Delta\omega_d(t) = \Delta\omega_d + at$$

will be fully concentrated without any spread, since here $s_f(t) = 0$. Note that $W_e(\omega)$ is the Fourier transform of window $w(t/2)w^*(-t/2)$ while $\Delta\omega_d$ without argument denotes the constant part of $\Delta\omega_d(t)$, i.e., $\Delta\omega_d = \Delta\omega_d(0)$.

4.1 Numerical implementation

Discrete version of (5) is

$$SM_L(k) = \sum_{i=-L}^{L} E(k+i)E^*(k-i)$$

or

$$SM_L(k) = SM_{L-1}(k) + 2\,\text{real}\{E(k+L)E^*(k-L)\}, \quad (6)$$

with $SM_0(k) = |E(k)|^2$ being the standard Fourier transform based representation.

Therefore, the S-method improvement can be achieved starting with the already obtained radar image, with additional simple matrix calculation according to (6).

5. EXAMPLES

Setup in [7] assumes: High resolution radar operating at the frequency $f_0 = 10.1$ GHz, bandwidth of linear FM chirps $B = 300$ MHz, pulse repetition frequency $f_r = 1/T_r = 2$ kHz with 2048 pulses in one revisit (image integration time $T_c \cong 2$ sec, cases with $T_c \cong 1$ sec and $T_c \cong 4$ sec are also considered). Pulse repetition time is $T_r = 0.5$ ms. The target is at 2 km distance from the radar, and rotates at $\omega_R = 4^0/\sec$. The nonlinear rotation with frequency $\Omega = 0.5$ Hz is superimposed, $\omega_R(t) = \omega_R + A\sin(2\pi\Omega t)$, and amplitude $A = 1.25^0/\sec$ corresponds to the total change in angular frequency ω_R for $2.5^0/$sec. Note that here range and cross-range resolutions are $R_{range} = c/(2B) = 0.5$ m, and $R_{cross-range} = \pi c/(\omega_0 T_c \omega_R) = 0.106$ m. Since no translation in the experiment exists, there is no need for translation compensation.

Assume that at $t = 0$ the line of points 1,2 and 3 is parallel to the line of sight Fig.1.

Signal model corresponding to one of 6 rotating parts is $d_p(t) = R + x_p\cos(\theta_R(t)) + y_p\sin(\theta_R(t))$ or after distance compensation

$$\begin{aligned} d_p(t) &= x_p\cos(\theta_R(t)) + y_p\sin(\theta_R(t)) \text{ with} \\ \theta'_R(t) &= \omega_R(t) = \omega_R + A\sin(2\pi\Omega t), \\ \theta_R(t) &= \omega_R t - A/(2\pi\Omega)\cos(2\pi\Omega t) + \phi_0 \end{aligned}$$

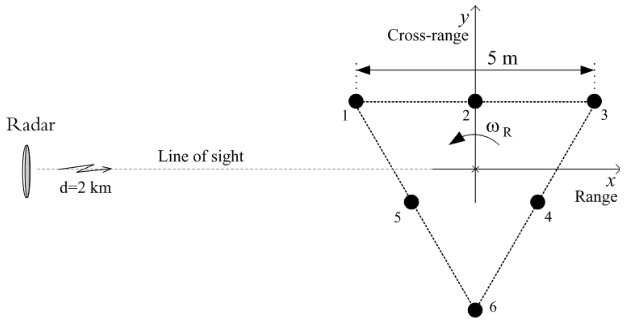

Figure 1: Illustation of the target simulation setup

we get the signal model with 6 components $q_p(m,t)$, each one of them being defined by (2) .

The obtained results are presented in Figs.2 for the instant $t = 9$ sec. Radar image in range/cross-range domain obtained by using: the Fourier transform (periodogram) and the S-method are given in these figures.

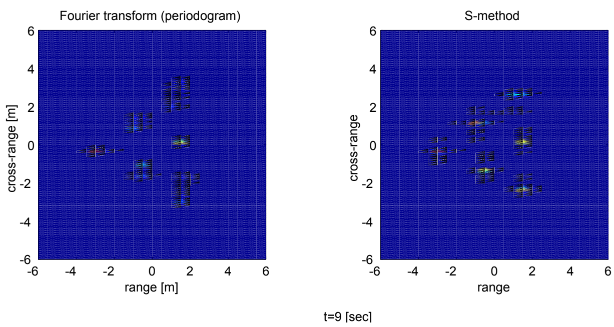

Figure 2: Radar image in range/cross-range domain: Periodogram (left), S-method(right) at the considered time instant $t = 9$sec.

5.1 Application to a three dimensional target model

Consider now the case when the target point at a position $\vec{r}$ rotates with an arbitrary oriented angular velocity $\vec{\omega}$. The angular velocity is decomposed into three axes oriented rotations defined by $(\omega_{rot}, \omega_{pitch}, \omega_{yaw})$. The corresponding angles of the target point are $(\theta_r(t), \theta_{pc}(t), \theta_y(t))$, where

$$\theta_i(t) = \int_0^t \omega_i(\tau)d\tau + \theta_i(0).$$

If $\vec{r} = (x_p, y_p, z_p)$ is the target position at $t = 0$ then at any other instant the position $\vec{r}' = (x_p', y_p', z_p')$ can be determined by using the rotation three-dimensional space matrix that reads [2] $\vec{r}' = R_{rot}(R_{pitch}R_{yaw})\vec{r}$. In this case distance from the radar at an instant t is

$$\begin{aligned} d(t) &= R(t) + \cos(\theta_{pc}(t))\cos(\theta_y(t))x_p \\ &\quad + \cos(\theta_{pc}(t))\sin(\theta_y(t))y_p - \sin(\theta_{pc}(t))z_p \end{aligned}$$

With $\theta_{pc}(t) = 0$ and $\theta_y(t) \equiv \theta_R(t)$ this model reduces to the two-dimensional model. In general, Doppler shift and ISAR image here assume much more complex form than in the 2D case.

Example: Consider the radar setup as in [7]. Assume here the same dimensions and parameters, but with a three dimensional rotation, instead of a 2D geometry, with

$$\omega_{yaw}(t) = \omega_R(t) = \omega_R + A\sin(2\pi\Omega t)$$

$\omega_R = 6^0/\sec$, $\Omega = 0.5$ and $A = 2^0/\sec$ and $B = 600$MHz. Assume also

$$\omega_{pitch}(t) = A_{pc}\cos(2\pi\Omega_{pc}t)$$

with $A_{pc} = 3^0/\sec$, $\Omega_p = 0.25$. The angle changes are

$$\begin{aligned} \theta_y(t) &= \theta_R(t) = \omega_R t - A/(2\pi\Omega)\cos(2\pi\Omega t) + A/(2\pi\Omega) \\ \theta_{pc}(t) &= A_{pc}/(2\pi\Omega_{pc})\sin(2\pi\Omega_{pc}t) \end{aligned}$$

Results as in the first Example, including the same comments, are shown in Fig.3.

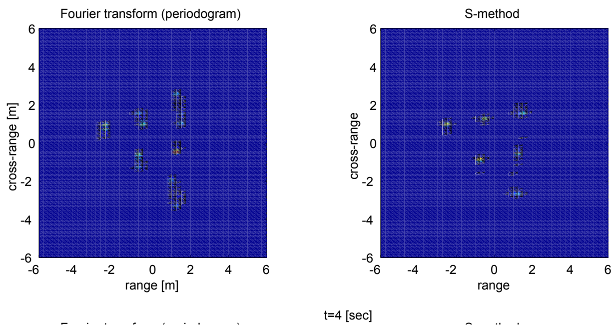

Figure 3: Radar image in range/cross-range domain: Periodogram (left), S-method(right) at the considered time instant $t = 4$sec.

5.2 Application to the boeing and mig target model

Finally, the presented method is applied to the model of boeing727 and mig, that are often used as standard benchmarks for the ISAR imaging methods. A simple virtual instrument realization form of the S-method is done according to (6). For $L = 0$ the standard Fourier transform based ISAR image is obtained. By changing the number of terms L we get the S-method based results with improved concentration of points, when movement has degraded the image resolution. The results are presented in Figs.4, 5, 6 and 7. The readability improvement obtained by using the S-method is evident.

6. CONCLUSION

A method for computationally simple improvement of ISAR images readability in the cases when they are blurred due to high target movement nonstationarities is presented. The method is based on the post processing of the whole set of data, its Fourier transform and time-frequency representation known as the S-method. The proposed method can improve the concentration almost as high as the Wigner distribution would do, but without or with reduced cross-terms. Accuracy analysis confirms the improvements in analytical and statistical way on a set of data produced according to the experimental setup used in literature for radar images analysis. A simple virtual instrument form of the S-method implementation in ISAR is presented and applied on typical signals representing radar images of boeing and mig.

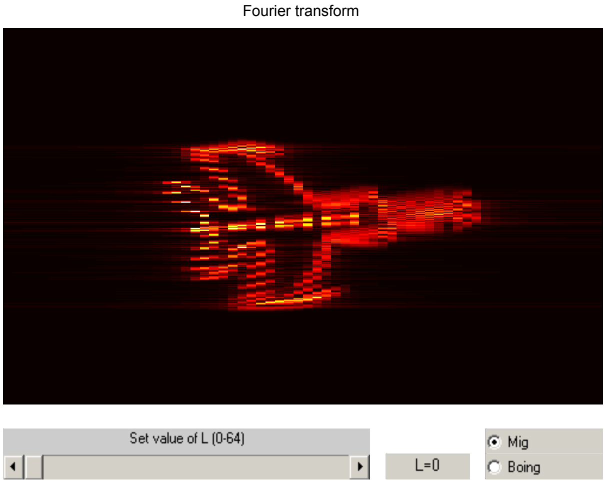

Figure 4: ISAR image of mig obtained by the Fourier transform (S-method with $L = 0$).

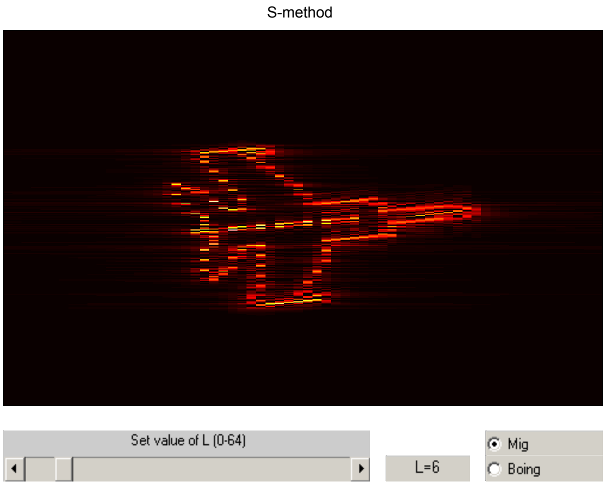

Figure 5: ISAR image of mig obtained by the Fourier transform improved by 6 additional terms (S-method with $L = 6$).

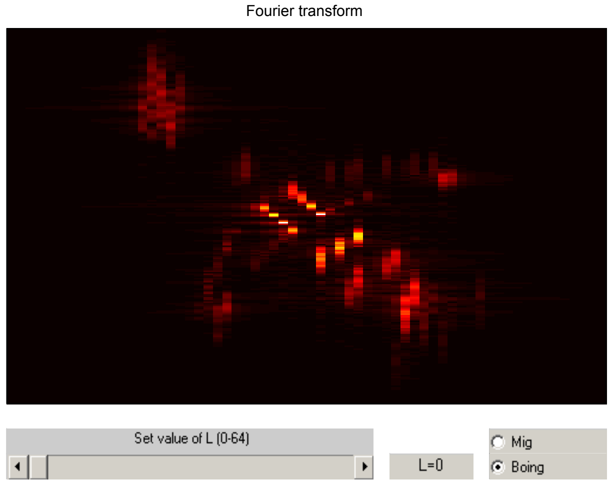

Figure 6: ISAR image of boing obtained by the Fourier transform.

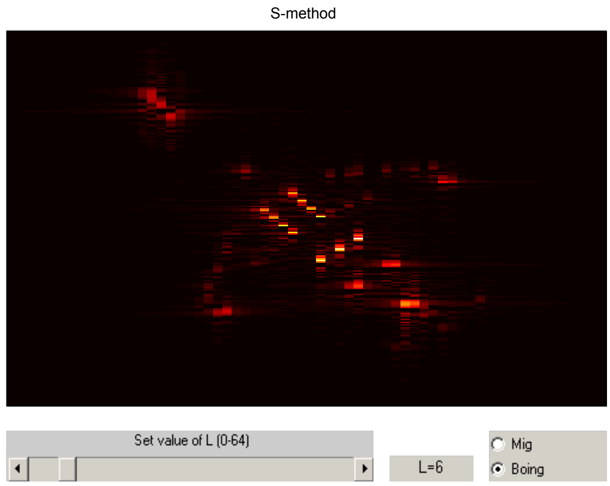

Figure 7: ISAR image of boing obtained by the Fourier transform improved by 6 additional terms (S-method with $L = 6$).

REFERENCES

[1] V. C. Chen, H. Ling, *Time-frequency transforms for radar imaging and signal analysis*, Artech Hoouse, 2002.

[2] V. C. Chen, W. J. Miceli, "Simulation of ISAR imaging of moving target", *IEE Proc.-Radar Sonar Navig.,* vol. 148, No. 3, June 2001, pp.160-166.

[3] S. Qian, D. Chen, *Joint time-frequency analysis: methods and applications*, Prentice-Hall Inc., New York, USA, 1996.

[4] L. L. Scharf, B. Friedlander, "Toeplitz and Hankel kernels for estimating time-varying spectra of discrete-time random processes," *IEEE Trans. Signal Processing*, vol. 49, pp. 179–189, 2001.

[5] LJ. Stanković, "A method for time-frequency analysis", *IEEE Trans. Signal Processing*, vol. 42, Jan. 1994, pp. 225-229.

[6] LJ. Stanković, J. F. Böhme, "Time-frequency analysis of multiple resonances in combustion engine signals," *Signal Processing,* vol.79, No. 1, pp.15-28, Nov.1999.

[7] T. Thayaparan, G. Lampropoulos, S. K. Wong, E. Riseborough, "Application of adaptive joint time-frequency algorithm for focusing distorted ISAR images from simulated and measured radar data", *IEE Proc. Radar, Sonar Navig.,* Vol.150, No. 4, Aug. 2003.

[8] Y. Wang, H. Ling, V. C. Chen, "ISAR motion compensation via adaptive joint time-frequency techniques", *IEEE Trans. Aerospace and Electronics Systems*, Vol. 43, No. 2, April 1988.